

Experimental Demonstration of Higher Precision Weak-Value-Based Metrology Using Power Recycling

Yi-Tao Wang,^{1,2} Jian-Shun Tang,^{1,2,†} Gang Hu,³ Jian Wang,^{1,2} Shang Yu,^{1,2} Zong-Quan Zhou,^{1,2}
Ze-Di Cheng,^{1,2} Jin-Shi Xu,^{1,2} Sen-Zhi Fang,³ Qing-Lin Wu,³
Chuan-Feng Li,^{1,2,*} and Guang-Can Guo^{1,2}

¹Key Laboratory of Quantum Information, University of Science and Technology of China, CAS, Hefei 230026, People's Republic of China

²Synergetic Innovation Center of Quantum Information Quantum Physics, University of Science and Technology of China, Hefei 230026, People's Republic of China

³Department of Physics, Central China Normal University, Wuhan 430079, People's Republic of China
(Received 9 June 2016; revised manuscript received 2 October 2016; published 29 November 2016)

The weak-value-based metrology is very promising and has attracted a lot of attention in recent years because of its remarkable ability in signal amplification. However, it is suggested that the upper limit of the precision of this metrology cannot exceed that of classical metrology because of the low sample size caused by the probe loss during postselection. Nevertheless, a recent proposal shows that this probe loss can be reduced by the power-recycling technique, and thus enhance the precision of weak-value-based metrology. Here we experimentally realize the power-recycled interferometric weak-value-based beam-deflection measurement and obtain the amplitude of the detected signal and white noise by discrete Fourier transform. Our results show that the detected signal can be strengthened by power recycling, and the power-recycled weak-value-based signal-to-noise ratio can surpass the upper limit of the classical scheme, corresponding to the shot-noise limit. This work sheds light on higher precision metrology and explores the real advantage of the weak-value-based metrology over classical metrology.

DOI: 10.1103/PhysRevLett.117.230801

Introduction.—Weak-value-based metrology has shown its great power in signal amplification since it was first introduced by Aharonov, Albert, and Vaidman in 1988 [1], based on the seminal work of the two-state-vector formalism of quantum mechanics [2]. In this weak-value-amplification (WVA) technique, the pre- and postselected ensemble play a critical role; therefore, it is also known as the postselected weak measurement [3]. To date, this WVA technique has been successfully employed in the measurement of some small physical effects, such as the optical spin Hall effect [4], beam deflections [5,6], phase shifts [7,8], plasmonic spin Hall effect [9], and angular rotations [10]. These experiments indicate that the WVA technique indeed benefits the measurement by suppressing the technical noise [11–13] and improves the corresponding precision. As a complex value, weak value always shows greater power in estimation precision when the imaginary part is utilized [5,7,11]. For example, in the interferometric weak-value-based beam-deflection measurement reported in Ref. [5], a purely imaginary weak value is obtained and the precision down to 400 ± 200 frad is reached, which corresponds to the linear travel of a piezoactuator down to 14 ± 7 fm, i.e., the order of the diameters of some large atomic nucleus.

However, in the technical-noise-free situation, considering the trade-off relation between the amplification effect and the probe loss induced by the postselection in this protocol, a direct question is raised of whether the WVA

technique can improve the ultimate limit of the measurement precision, i.e., to go beyond the signal-to-noise ratio (SNR) or Fisher information corresponding to the shot-noise limit. This question has stimulated many discussions recently [13–15], and it has been shown that weak value offers no precision advantages in the ideal scenario [14,15], no matter when the real or imaginary part is utilized. Particularly, in the interferometric beam-deflection measurements [5], this standard weak-value-based protocol does not provide a higher precision limit, compared with that of the classical measurement protocol (SNR corresponding to shot noise) in which the beam is directly focused onto the detector [12,13]. It seems that the probe loss caused by the postselection plays the critical role in this problem. Therefore, some recent works theoretically propose to reduce this critical probe loss by the utilization of the recycling technique [16,17], especially the power-recycling technique, which has been successfully applied in the detection of gravitational waves [18,19].

The logic diagram for the power-recycled weak-value-based (PRWV) metrology compared with that of the classical and standard weak-value-based (SWV) metrologies is shown in Fig. 1, in which a physical effect of the target system is measured. The classical metrology usually contains the following processes [20]: first, the preparation of the probe; second, the interaction process (in this work we only focus on the weak-interaction situation) during which some physical quantities of the probe couple to the

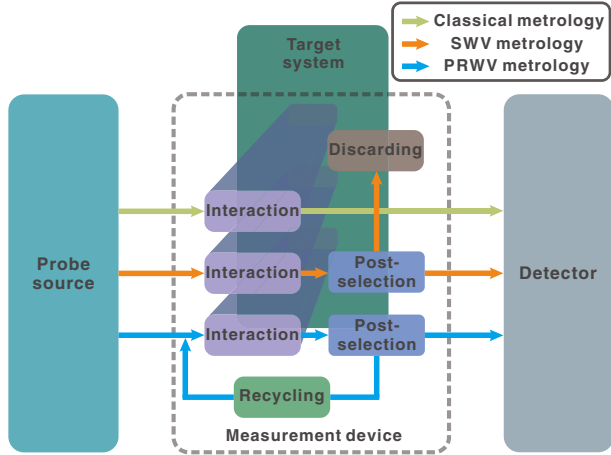


FIG. 1. The schematic diagram of three metrological protocols. The classical metrology is constituted by three steps: the probe preparation, the interaction between the probe and the target system (in this work, we focus on the weak-interaction situation), and the probe detection. For the weak-value-based metrologies, an additional step of probe postselection is inserted. The probe that is not postselected is discarded in the SWV metrology, and is, however, recycled in the PRWV metrology. The steps in the dashed box can be regarded as the measurement devices, which output the results of the probe coupling to the target system, which are then detected by the detector.

system parameter; third, the probe detection; and finally, the parameter estimation according to the detected probe quantities (not shown in Fig. 1). By inserting an additional step of postselection after the interaction, the SWV metrology can obtain an amplified weak value instead of the expectation value in the classical metrology. However, it has to undergo the loss of probe, which will decrease the measurement precision [15]. An optimal weak-value-based metrology should make full use of the wasted probe; therefore, an improved idea is to recycle the probe that is supposed to be discarded. This strategy is the PRWV metrology. Taking the probe source and the detector in Fig. 1 as the invariant input and output devices, respectively, different measurement outcomes will be obtained when different measurement devices (the dashed box in Fig. 1) are used. The classical and the SWV protocols have the advantages of either the large data amount or the amplified physical effect, while the PRWV protocol can combine both of the advantages together [16,17].

In this work, we experimentally study the precision problem in the interferometric weak-value-based beam-deflection measurement using both the SWV and PRWV strategies [17] and compare the measurement precision of the SWV and PRWV (and also the classical) strategies. For the PRWV strategy, we place a partially transmitting mirror at the bright port of the interferometer (on the basis of the SWV configuration) to form a resonant cavity, which sends the unpostselected photons back into the measurement device, and the number of the detected photons at the dark

port will receive a gain, i.e., the decrease of the probe loss. Meanwhile, the amplification effect of the weak value remains nearly unchanged. Therefore, the ultimate precision of the PRWV protocol can be increased and can surpass the precision limit of the SWV protocol (and also the classical protocol, which has been examined experimentally). To avoid the effect of the technical noise, we use the discrete Fourier transform (DFT) method to extract the signal and white noise (dominated by shot noise) in the data processing. Our results show that the detected signal (proportional to the beam deflection) is amplified by a gain factor of 2.40 ± 0.12 in our PRWV measurement compared to the SWV scheme. Moreover, the SNR related to the white noise in our PRWV measurement indeed surpasses the SNR limit of the SWV and classical schemes. These results indicate that the WVA metrology shows an obvious measurement-precision advantage over the classical metrology when the power-recycling technique is combined.

Theoretical framework.—For the SWV protocol, a probe beam is injected into the measurement device (the Sagnac interferometer in Fig. 2) without the cavity mirror. In this interferometer, the piezo-driven beam splitter (BS) induces a beam momentum shift $k = k_0 \varepsilon$ on the reflected beam, with k_0 denoting the probe light's wave number and ε denoting the beam-deflection angle (in rad). Under the weak-value condition $kD \ll \phi/2 \ll 1$ (D represents the beam size and ϕ is the phase delay between the clockwise and the counterclockwise beam), the postselection probability is expressed as $P_{ps} = \sin^2(\phi/2) \approx (\phi/2)^2$ and only a small fraction of photons can exit from the dark port of the interferometer. The momentum shift then results in an amplified position-expectation shift $\langle \Delta x \rangle \approx k\sigma^2/(2\phi)$ on the dark-port output beam, which is related to the imaginary weak value (σ represents the $1/e$ diameter of the Gaussian beam) [12,21]. This position shift can be estimated by detecting the photon number difference between the left and right sides of the output beam. Compared to the classical scheme in which the beam is directly focused onto the detector by a lens (the focal length is f_c) and the beam position shift is $\langle \delta \rangle = f_c k/k_0$, the amplification factor is $\langle \Delta x \rangle / \langle \delta \rangle \approx k_0 \sigma^2 / (2\phi f_c)$.

By using the knife-edge prism (KEP) to split the beam into two halves and coupling both halves into the single-photon avalanche diodes (SPADs), respectively, the photon number difference s per unit time can be counted. The average difference is given by $\langle s \rangle \approx 2N_{det} k\sigma / (\phi\sqrt{\pi})$ in the case of the collimated beam, where N_{det} is the total photon number detected per unit time [17]. For the convergent case in our setup, a multiplicative factor of $F = (f - l_{lb})/f$ should be applied where f is the focal length of $L3$ and $L4$ and l_{lb} represents the distance between $L3$ and the 50:50 BS (or equivalently, the distance between $L4$ and the BS). The details of the calculations for F are shown in Supplemental Material [22]. Thus, the shot-noise-limited SNR can be derived as

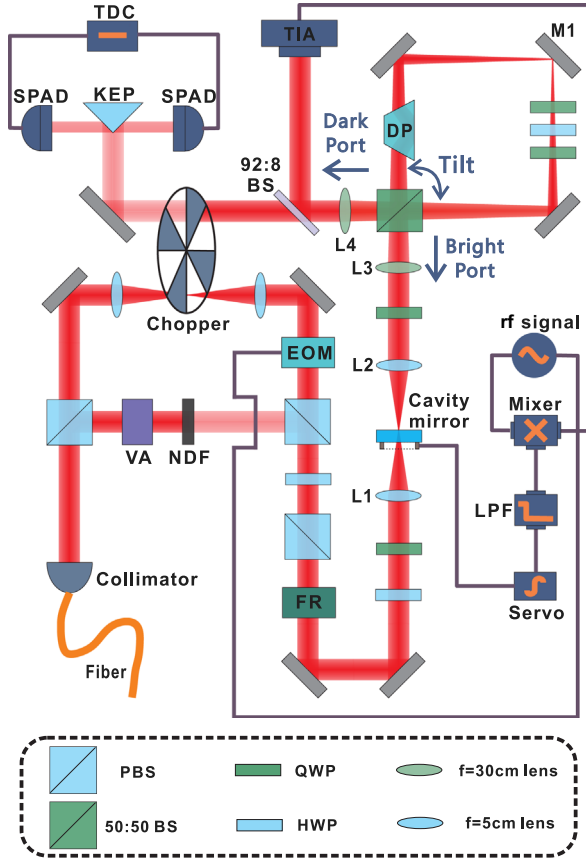


FIG. 2. Experimental setup of the power-recycled weak-value-based beam-deflection measurement. This setup is constituted by four parts: the probe source, the measurement device, the splitting detector, and the PDH system used to stabilize the cavity length. The probe source is the beam attenuated by the neutral-density filter (NDF). This beam is focused onto the cavity mirror and sent into the measurement device. The measurement device consists of a cavity mirror and a Sagnac interferometer. The beam deflection is imposed via a piezo-driven 50:50 BS and is coupled to the transverse beam position when exiting from the dark port. The splitting detector is realized using a KEP, two SPADs, and a time-to-digital converter (TDC), which is used to detect the beam-position shift. The PDH system contains the reference beam modulated by the chopper, the transimpedance amplifier (TIA) used to detect the power of this beam, the following signal-processing circuits, and the servo to stabilize the cavity mirror. LPF, low-pass filter; M1, mirror 1; DP, dove prism; FR, Faraday rotator; EOM, electro-optic modulator; PBS, polarizing beam splitter; VA, variable attenuator; QWP, quarter-wave plate; HWP, halfwave plate.

$$R = \frac{\langle s \rangle}{\sqrt{N_{\text{det}}}} \approx \frac{2Fk\sigma}{\phi\sqrt{\pi}} \sqrt{N_{\text{det}}}. \quad (1)$$

In the PRWV protocol, the power recycling is realized by inserting the cavity mirror at the bright port of the interferometer (see Fig. 2) to form a resonant cavity with the assistance of this Pound-Drever-Hall (PDH) system and performs the optimal recycling for the unpostselected probe photons. The power gain factor inside the cavity can be expressed as $G = (1 - r) / [1 + (1 - \beta)r - 2\sqrt{r(1 - \beta)}]$,

where r is the reflectivity of the cavity mirror and β is the power-loss factor during one traversal in the cavity [22]. In the ideal situation, the only loss in this cavity is caused by the postselection, whereas in the practical situation, there are some other losses induced by, for example, the imperfect transmittivity or reflectivity of the optical components. In our experiment, the one-traversal loss factor β is approximately 0.4 and the postselection probability is 10%. A cavity mirror with a reflectivity of 70%, which matches the loss, is used here to acquire the optimal power gain. The probe utilization ratio can be boosted through this cavity-enhancement method, and the detected photon number is also increased to GN_{det} .

Experiment.—The experimental setup is sketched in Fig. 2, which can be recognized as four parts: (1) the probe source, which supplies the single-photon-level probe beam for the measurement task, (2) the measurement device, which couples the beam deflection to the output beam's transverse position, (3) the splitting detector, which detects the beam-position shift, and (4) the PDH system [23,26], which stabilizes the cavity length according to the detected signal from the reference beam (~ 2 mW). In order to evaluate the SNR result originated from the shot noise, the power of the probe beam is attenuated to the single-photon level, and the effect of the technical noise can be relatively small. This beam is finally detected by the SPADs in the splitting detector. To further reduce the effect of the technical noise, we use the DFT method to extract the difference signal (proportional to the beam deflection) and the white noise (dominated by the shot noise). The details of the experimental setup (including the PDH signal analysis) and the data processing can be found in the Supplemental Material [22].

Figure 3 shows the relation between the various angles of the beam deflection (in rad) and the average difference signal ($\overline{s_0}$), which is derived through the data processing including the DFT method [22]. The red dots are obtained in the power-recycled configuration, and the blue triangles are obtained when the cavity mirror is removed. The detected total photon count is 84.02 ± 0.03 per integration time in the case of the absence of the cavity mirror. The red solid and blue dashed lines are derived by linearly fitting on these average difference signals, and the ratio between the slopes of these lines is 2.40 ± 0.12 . This result shows that the power-recycled signal can be boosted to 2.40 ± 0.12 times of that in the standard situation, and the average difference signal still keep linear with respect to the deflection angle in the power-recycled situation.

The SNR related to the shot noise can be estimated as $R = \overline{s_0} / \overline{\mu}$, where $\overline{\mu}$ is the average white noise derived in the frequency domain of the detected difference count (see details for $\overline{\mu}$ in the Supplemental Material [22]), which is equal to the SNR derived by Eq. (1) in the technical-noise-free situation. To compare the measurement precisions of the weak-value-based and classical metrologies, the classical-strategy-based experiment is also performed and

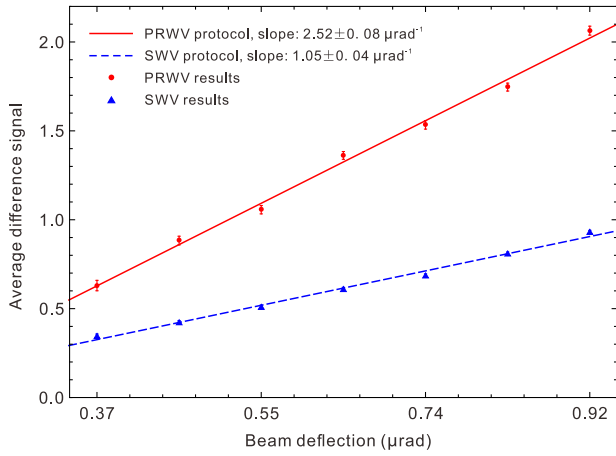


FIG. 3. The relations between the average difference signal \bar{s}_0 (of 260 sample sequences) and the beam deflection in the PRWV and SWV situations. The red solid and blue dashed lines are the linear-fit results of the corresponding experimental results. The slopes indicate that the difference signal is amplified by a factor of 2.40 ± 0.12 after combining the power-recycling technique. The error bars correspond to the standard error of the results.

the corresponding SNR is evaluated, which should be equal to the SNR of the SWV protocol in the ideal situation [12,13]. The details about the classical-strategy-based experiment can be found in the Supplemental Material [22]. The numbers of the input probe photons are all the same for the classical-, SWV-, and PRWV-strategy-based experiments. The SNR results are shown in Fig. 4(a). The beam-deflection angle here is $\varepsilon = 0.92 \mu\text{rad}$. The blue triangles, red dots, and orange squares are the results for the SWV, PRWV, and classical protocols, respectively. All the SNR results increase with the input probe photon number. The shot-noise-limited SNR for the SWV protocol (blue dashed line) is derived from Eq. (1), which is lower than that for the classical protocol (orange solid line; details for the derivation of this line are presented in the Supplemental Material [22]). This is caused by the negative effects appearing in the practical SWV experiment: the additional probe loss introduced by more optical components in the SWV configuration, the uncollimated beam (which makes $F < 1$), etc. The difference between the SWV (classical) result and its (corresponding) shot-noise-limited SNR line in Fig. 4(a) is caused by the effect of the background photons, which make no contribution to the signal but bring in additional shot noise. The light orange region represents the confidence interval of the classical shot-noise-limited SNR under the level of 0.999, which is entirely below the PRWV data. This indicates that the PRWV protocol indeed shows the advantage of the measurement precision even when not considering the suppression effect of the residual technical noises, and the WVA technique in the power-recycling configuration can surpass the shot-noise limit of the classical technique. Figures 4(b) and 4(c) show the derived white noises in the SWV and classical protocols, respectively, using blue dots,

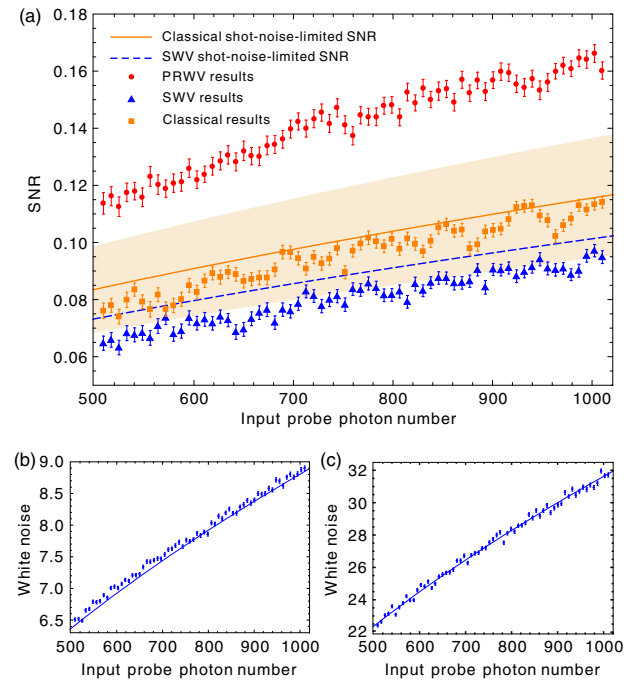


FIG. 4. (a) The relation between the white-noise-related SNR and the input probe photon number per integration time for the classical, SWV, and PRWV protocols. The orange solid and blue dashed lines are the shot-noise-limited SNR of the classical and SWV protocols, respectively. The light orange region is the confidence interval of the classical shot-noise-limited SNR under the level of 0.999. These results indicate that the SNR of the PRWV protocol surpasses the classical limit under the confidence level of 0.999. (b),(c) The relation between the white noise and the input probe photon number in the (b) SWV and (c) classical protocols. The dots represent the experimental data, and the lines show the shot noises, which are calculated from the square roots of the detected photon numbers per integration time. The error bars correspond to the standard error of the results.

and the corresponding lines are the shot noises calculated from the square roots of the detected photon numbers. The tiny differences between the experimental results and the corresponding shot-noise lines show that the white noises other than shot noise included in the data should be less than 1%, which may be the technical noises originated from the afterpulsing effect and the detecting-efficiency jitter of the SPADs.

Conclusions.—We have demonstrated a proof-of-principle experiment of power-recycled interferometric weak-value-based beam-deflection measurement, which provides a practical way to recycle the wasted probe in the WVA technique. We investigate the measurement ability of the PRWV protocol, which can increase the SNR beyond the precision limit corresponding to the shot noise in the SWV and classical schemes (in the same conditions for the probe source and detectors). It indicates that the WVA technique indeed shows the advantage with a higher measurement precision by appropriately utilizing

the wasted probes. In addition, in the practical perspective, this power-recycling scheme can also further suppress the influence of some common technical noises, such as the constant background noise induced by the often-used electrical detectors, because of the further amplification of the strength of the detected signal. Although the PRWV protocol is demonstrated here in the situation of the interferometric beam-deflection measurement, it is very suitable to be transplanted to many other weak-value-based experiments, since the probe wasting by postselection is ubiquitous in all the SWV experiments. These properties make the PRWV protocol exhibit a great advantage in the improvement of the measurement precision.

Besides the power-recycling technique used in the PRWV protocol, there are also some other interesting techniques that are used to increase the measurement precision. For the pulsed-probe-source situation, the multibounce pulse-recycling strategy is another choice to solve the probe-loss problem in the weak-value-based metrology [16,27]. Also, various enhancement methods in other metrologies can be brought in for higher measurement precision by enhancing the interaction process. Kasevich's group introduces a multibounce mirror into the weak-value-based beam-deflection measurement to make the probe interact with the target system for multiple times [6]. They realize the multiple-interaction scheme with around ten bounces and show the enhancement to the angular sensitivity, which is in principle proportional to the number of bounces. The combination of this multiple-interaction technique and the power-recycling technique could further enhance the measurement precision. In addition, some quantum metrology could also be combined with the PRWV metrology to obtain higher measurement precision, such as entanglement-assisted WVA [28] and using a quantum probe source [3,24]. These techniques will shed light on the development of metrologies with ultrahigh precisions.

This work is supported by the National Natural Science Foundation of China (Grants No. 61490711, No. 11304305, No. 11674304, No. 11274289, No. 11474267, No. 11325419, No. 61327901, and No. 91321313), the Strategic Priority Research Program(B) of the Chinese Academy of Sciences (Grant No. XDB01030300), the Fundamental Research Funds for the Central Universities (No. CCNU 15A02036), and the Key Research Program of Frontier Sciences of the Chinese Academy of Sciences (Grant No. QYZDY-SSW-SLH003).

* cfli@ustc.edu.cn

† tjs@ustc.edu.cn

- [1] Y. Aharonov, D. Z. Albert, and L. Vaidman, *Phys. Rev. Lett.* **60**, 1351 (1988).
 [2] Y. Aharonov, P. G. Bergmann, and J. L. Lebowitz, *Phys. Rev.* **134**, B1410 (1964).
 [3] S. Pang and T. A. Brun, *Phys. Rev. Lett.* **115**, 120401 (2015).

- [4] O. Hosten and P. Kwiat, *Science* **319**, 787 (2008).
 [5] P. B. Dixon, D. J. Starling, A. N. Jordan, and J. C. Howell, *Phys. Rev. Lett.* **102**, 173601 (2009).
 [6] J. M. Hogan, J. Hammer, S.-W. Chiow, S. Dickerson, D. M. S. Johnson, T. Kovachy, A. Sugarbaker, and M. A. Kasevich, *Opt. Lett.* **36**, 1698 (2011).
 [7] X.-Y. Xu, Y. Kedem, K. Sun, L. Vaidman, C.-F. Li, and G.-C. Guo, *Phys. Rev. Lett.* **111**, 033604 (2013).
 [8] N. Brunner and C. Simon, *Phys. Rev. Lett.* **105**, 010405 (2010).
 [9] Y. Gorodetski, K. Y. Bliokh, B. Stein, C. Genet, N. Shitrit, V. Kleiner, E. Hasman, and T. W. Ebbesen, *Phys. Rev. Lett.* **109**, 013901 (2012).
 [10] O. S. Magaña-Loaiza, M. Mirhosseini, B. Rodenburg, and R. W. Boyd, *Phys. Rev. Lett.* **112**, 200401 (2014).
 [11] Y. Kedem, *Phys. Rev. A* **85**, 060102 (2012).
 [12] G. I. Viza, J. Martínez-Rincón, G. B. Alves, A. N. Jordan, and J. C. Howell, *Phys. Rev. A* **92**, 032127 (2015).
 [13] A. N. Jordan, J. Martínez-Rincón, and J. C. Howell, *Phys. Rev. X* **4**, 011031 (2014).
 [14] C. Ferrie and J. Combes, *Phys. Rev. Lett.* **112**, 040406 (2014).
 [15] G. C. Knee and E. M. Gauger, *Phys. Rev. X* **4**, 011032 (2014).
 [16] J. Dressel, K. Lyons, A. N. Jordan, T. M. Graham, and P. G. Kwiat, *Phys. Rev. A* **88**, 023821 (2013).
 [17] K. Lyons, J. Dressel, A. N. Jordan, J. C. Howell, and P. G. Kwiat, *Phys. Rev. Lett.* **114**, 170801 (2015).
 [18] B. P. Abbott *et al.*, *Rep. Prog. Phys.* **72**, 076901 (2009).
 [19] J. Abadie *et al.* (LIGO Scientific Collaboration), *Nat. Phys.* **7**, 962 (2011).
 [20] V. Giovannetti, S. Lloyd, and L. Maccone, *Phys. Rev. Lett.* **96**, 010401 (2006).
 [21] J. C. Howell, D. J. Starling, P. B. Dixon, P. K. Vudyaasetu, and A. N. Jordan, *Phys. Rev. A* **81**, 033813 (2010).
 [22] See Supplemental Material at <http://link.aps.org/supplemental/10.1103/PhysRevLett.117.230801>, which includes Refs. [6,16,17,21,23,24,25], for the experimental details and theoretical derivations.
 [23] E. D. Black, *Am. J. Phys.* **69**, 79 (2001).
 [24] J. W. Goodman, *Introduction to Fourier Optics*, 3rd ed. (Roberts & Company, Greenwood Village, CO, 2005).
 [25] J. W. Goodman, *Statistical Optics* (John Wiley & Sons, Inc., New York, 2000).
 [26] R. W. P. Drever, J. L. Hall, F. V. Kowalski, J. Hough, G. M. Ford, A. J. Munley, and H. Ward, *Appl. Phys. B* **31**, 97 (1983).
 [27] C. Byard, T. Graham, A. Jordan, and P. G. Kwiat, in *Proceedings of Frontiers in Optics, San Jose, CA, 2015* (The Optical Society of America, Washington, DC, 2015), paper JW2A.69; in *Proceedings of Research in Optical Science, Berlin, 2014* (The Optical Society of America, Washington, DC, 2014), paper QTh4A.3; in *Proceedings of CLEO: QELS Fundamental Science, San Jose, CA, 2014* (The Optical Society of America, Washington, DC, 2014), paper FF1D.8.
 [28] S. Pang, J. Dressel, and T. A. Brun, *Phys. Rev. Lett.* **113**, 030401 (2014).
 [29] V. Giovannetti, S. Lloyd, and L. Maccone, *Science* **306**, 1330 (2004).